Intravoxel incoherent motion imaging has the possibility to detect liver abnormalities in young Fontan patients with good hemodynamics

Kazuhiro Shiraga[1,2] , Kojiro Ono[3,4], Ryo Inuzuka[2], Hiroko Asakai[2], Takumi Ookubo[3], Akira Shirayama[3], Kouji Higashi[1] and Hiromichi Nakajima[1]

[1]Department of Cardiology, Chiba Children's Hospital, Chiba, Japan; [2]Department of Pediatrics, The University of Tokyo Hospital, Bunkyo-ku, Tokyo, Japan; [3]Department of Radiology, Chiba Children's Hospital, Chiba, Japan and [4]Division of Fundamental Engineering, Graduate School of Science and Engineering, Chiba University, Chiba, Japan

Abstract

Introduction: Liver fibrosis and cirrhosis are one of the critical complications in Fontan patients. However, there are no well-established non-invasive and quantitative techniques for evaluating liver abnormalities in Fontan patients. Intravoxel incoherent motion diffusion-weighted imaging with MRI is a non-invasive and quantitative method to evaluate capillary network perfusion and molecular diffusion. The objective of this study is to assess the feasibility of intravoxel incoherent motion imaging in evaluating liver abnormalities in Fontan children. *Materials and Methods:* Five consecutive Fontan patients and four age-matched healthy volunteers were included. Fontan patients were 12.8 ± 1.5 years old at the time of MRI scan. Intravoxel incoherent motion imaging parameters (D, D*, and f values) within the right hepatic lobe were compared. Laboratory test, ultrasonography, and cardiac MRI were also conducted in the Fontan patients. Results of cardiac catheterization conducted within one year of the intravoxel incoherent motion imaging were also examined. *Results:* In Fontan patients, laboratory test and liver ultrasonography showed almost normal liver condition. Cardiac catheter and MRI showed good Fontan circulation. Cardiac index was 2.61 ± 0.23 L/min/m². Intravoxel incoherent motion imaging parameters D, D*, and f values were lower in Fontan patients compared with controls (D: 1.1 ± 0.0 versus $1.3 \pm 0.2 \times 10^{-3}$ mm²/second (p = 0.04), D*: 30.8 ± 24.8 versus $113.2 \pm 25.6 \times 10^{-3}$ mm²/second (p < 0.01), and f: 13.2 ± 3.1 versus $22.4 \pm 2.4\%$ (p < 0.01), respectively). *Conclusions:* Intravoxel incoherent motion imaging is feasible for evaluating liver abnormalities in children with Fontan circulation.

Introduction

Liver fibrosis and cirrhosis are one of the critical complications in Fontan patients. In adult patients with normal heart structure, there are multiple methods to evaluate parenchymal liver abnormalities, including ultrasonography, contrast-enhanced computed tomography, biopsy, and elastography. However, there have been no well-established non-invasive and quantitative techniques to evaluate liver abnormalities in Fontan patients. Transient ultrasound elastography and magnetic resonance elastographies are prevalently used to assess liver fibrosis because they are non-invasive and quantitative techniques. However, fibrosis assessed by elastography can be overestimated with elevated central venous pressure, which is a major limitation in using elastography in Fontan patients.[1–4]

Intravoxel incoherent motion diffusion-weighted imaging is a non-invasive and quantitative method for the assessment of diffuse liver disease. Intravoxel incoherent motion imaging was initially described by Le Bihan et al in brain imaging.[5–8] They defined intravoxel incoherent motion as the microscopic translational motions that occur in each image voxel in MRI. In biological tissues, signal decay with an intravoxel incoherent motion diffusion-weighted imaging sequence follows a biexponential curve, which accounts for a double component of diffusion – presumably, pure molecular diffusion and perfusion-related diffusion. Therefore, intravoxel incoherent motion imaging can measure the values related to pure molecular diffusion affected by histological structure and capillary network perfusion, separately.[5–7,9–15]

Liver fibrosis and cirrhosis are associated with extracellular matrix accumulation, which may affect both capillary perfusion and diffusion. Thus, intravoxel incoherent motion imaging is being recognised as a sensitive way to detect structural and perfusion abnormalities in fibrotic and cirrhotic livers in the setting of normal heart structure. Intravoxel incoherent motion imaging has been successfully applied to the assessment of liver fibrosis and cirrhosis in adult patients with normal heart structure.[10,16–20]

Intravoxel incoherent motion imaging may be a potential tool for detecting liver abnormalities without being affected by central venous pressure in patients with Fontan circulation.

Dijkstra et al showed the feasibility of intravoxel incoherent motion imaging in young adult Fontan patients (mean-age, 19 years) compared with healthy adults (mean-age, 33 years).[21] It remains unclear that how intravoxel incoherent motion imaging values differ in children with Fontan circulation compared to healthy children. The objective of this study is to assess the feasibility of intravoxel incoherent motion imaging for evaluating liver abnormalities in Fontan children.

Materials and Methods

Patients

This prospective study was approved by our institutional Research and Ethics Committee and written informed consent was obtained from all patients. We enrolled five consecutive Fontan patients at our outpatient clinic. Four age-matched healthy volunteers were included as controls. In Fontan patients, blood examination, liver ultrasonography, cardiac MRI, and intravoxel incoherent motion imaging were conducted. In control patients, only liver intravoxel incoherent motion imaging was conducted.

Cardiac function analysis

During a cardiac MRI, phase-contrast flow volume analyses at inferior caval vein and superior caval vein were conducted. The sum of these flow volumes was considered for systemic blood flow. Quantitative flow measurements from phase-contrast images were obtained with spontaneous breathing to avoid change in hemodynamic status. The results of cardiac catheterization conducted within 1 year of the intravoxel incoherent motion imaging were also reviewed.

Liver function analysis (blood examination, ultrasonography)

Laboratory testing assessed included platelet count, total bilirubin, aspartate aminotransferase, alanine aminotransferase, gamma-glutamyl transpeptidase, hyaluronic acid, procollagen III N-terminal peptide, type IV collagen 7s, and brain natriuretic peptide. Liver size, form, margin, abnormal lesion, portal vein, and hepatic vein flow were assessed with liver ultrasonography.

Liver intravoxel incoherent motion imaging and analysis

All MRI was performed with a 1.5 Tesla MRI scanner; Signa HDxt Ver. 23 with 8-Channel cardiac coil (GE Healthcare, Milwaukee, United States of America). MRI was performed after more than 2 hours of fasting to avoid the change of portal blood flow during food digestion.

The intravoxel incoherent motion imaging sequence was performed by using respiratory triggered single-shot echo-planar imaging spin-echo sequence with 11 b values (parameters in Table 1). Circular region of interests with 26.5 mm diameter each was placed manually in each right lobe among Segments 5–8, putting aside extrahepatic fat, large hepatic vessels, and large bile ducts. The left hepatic lobe was excluded due to potential cardiac motion artifacts that could interfere with accurate measurement of intravoxel incoherent motion imaging parameters.[16] The recorded signal intensity was obtained at each b value by averaging the mean signal intensity in each region of interest.

According to intravoxel incoherent motion imaging theory,[5–8] the biexponential model fitting was used to calculate the signal attenuation as a function of b as follows:

Table 1. Intravoxel incoherent motion imaging parameters.

Parameter	Value
Scan plane	Axial
Repetition time (ms)	6000 ~ 11250
Echo time (ms)	75.2
b-values (s/mm^2)	0, 10, 20, 30, 50, 80, 100, 200, 400, 800, 1000
Field of view (mm)	300
Slice thickness (mm)	7
Slice gap (mm)	1.5
Parallel imaging factor	ASSET: 2
Pixel bandwidth (Hz/pixel)	1953.1
Number of averages	1–4
Acquisition matrix	128 × 192

$$SI_b = SI_0[(1-f) \times \exp^{-b \times D} + f \times \exp^{-b \times (D^* + D)}] \quad (1)$$

where SI_b is the signal intensity at a given b value and SI_0 is the signal intensity for $b = 0$ second/mm^2 and is proportional to $\exp^{-TE/T2}$, respectively. In this scanning protocol, we scanned liver on diffusion-weighted imaging first, and we analysed intravoxel incoherent motion imaging values off-line after scan. Within a single scan, three intravoxel incoherent motion imaging values (D, D*, and f values) are calculated. D value reflects pure molecular diffusion, which is affected by changes in cell density and histological structure.[5,6,10] A decreased D value in chronic liver disease reflects an increase in connective tissue, which changes the cell density and histological structure.[19] D* is the pseudo-diffusion coefficient representing the capillary perfusion within the voxel, and f is the perfusion fraction related to the capillary perfusion. Both D* and f values are surrogate markers of capillary liver perfusion,[10] and a decreased D* or f value reflects decreased capillary perfusion. Dijkstra et al showed that D* and f values in liver reflect capillary perfusion in a way resembling contrast-enhanced MRI.[20]

Intravoxel incoherent motion imaging parameters (D, D*, and f values) were calculated by using a partially constrained non-linear regression algorithm based on equation (1). All regression algorithms were based on least-square fits and performed with Osirix DICOM Viewer (Pixmeo SARL, Geneva, Switzerland) plugin tool; ADC Map Calculation (Stanford University, California, United States of America). The D, D*, and f values were averaged over Segments 5–8.

Statistical analysis

Data are described as mean ± standard deviation. Comparison of intravoxel incoherent motion imaging parameters between Fontan patients and controls were performed using a student t-test. Heterogeneity of intravoxel incoherent motion imaging parameters among Segments 5–8 was assessed using analysis of variance (ANOVA). Statistical significance was defined as a p value of less than 0.05. Statistical analyses were performed using JMP 9 (SAS Institute Inc., Cary, United States of America).

Results

Patients' characteristics are shown in Table 2. There were no significant differences between Fontan patients and controls in

Table 2. Fontan patients' characteristics.

	Age (years)	Gender	Height (cm)	Weight (kg)	Diagnosis	Method of Fontan	Age at Fontan surgery
Fontan 1	11	F	147	38	SRV	ECLT	2 years
Fontan 2	12	M	126	27	PA/IVS	ECLT	2 years
Fontan 3	12	M	150	54	TA	ECLT	3 years
Fontan 4	14	F	138	30	Ebstein	ECLT	2 years
Fontan 5	15	M	163	51	HLHS	Atrial flap	3 years

Ebstein = Ebstein's anomaly, ECLT = extracardiac lateral tunnel, F = Female, HLHS = hypoplastic left heart syndrome, M = male, PA/IVS = pulmonary atresia with intact ventricular septum, SRV = single right ventricle, TA = tricuspid atresia.

age: 12.8 ± 1.5 versus 10.0 ± 1.9 (p = 0.06), height: 144.7 ± 13.8 versus 137.5 ± 11.7 cm (p = 0.46), and weight: 40.0 ± 12.4 versus 32.4 ± 9.6 kg (p = 0.37). There were three males and two females in Fontan patients, and four males in controls. The underlying cardiac diagnoses in the Fontan patients were pulmonary atresia and intact ventricular septum (1 patient), tricuspid atresia (1 patient), Ebstein's anomaly (1 patient), and hypoplastic left heart syndrome (2 patients). Fontan surgery was performed at age 2.6 ± 0.5 years old, and the intravoxel incoherent motion imaging was performed 10.5 ± 1.5 years after Fontan surgery. All patients were NYHA class I.

In Fontan patients, laboratory test showed no overt abnormalities in liver condition, fibrotic markers and brain natriuretic peptide values (Table 3). All patients were Child-Pugh score A. Liver ultrasonography demonstrated normal liver size, form, margin, abnormal lesion, portal vein and hepatic vein flow in four patients, and only one patient showed slightly dilated hepatic veins with normal other factors. Cardiac catheterization and MRI for Fontan patients showed good Fontan circulation. The cardiac index was 2.61 ± 0.23 L/min/m^2, central venous pressure was 10.2 ± 1.3 mmHg, and pulmonary vascular resistance was 1.15 ± 0.27 U $\times$ m^2.

Intravoxel incoherent motion imaging parameters of liver among Segments 5–8 in Fontan patients and controls are shown in Table 4 (individual data are shown in Supplementary table 1). We compared each intravoxel incoherent motion imaging parameters averaged over Segments 5–8 between two groups. The average values in Fontan patients were significantly lower than controls in D: 1.1 ± 0.0 versus $1.3 \pm 0.2 \times 10^{-3}$ mm^2/second (p = 0.04), D*: 30.8 ± 24.8 versus $113.2 \pm 25.6 \times 10^{-3}$ mm^2/second (p < 0.01), and f: 13.2 ± 3.1 versus $22.4 \pm 2.4\%$ (p < 0.01) (Fig 1). No significant difference in intravoxel incoherent motion imaging parameters was detected among each Segment in Fontan patients: p = 0.49 for D, p = 0.52 for D*, and p = 0.15 for f; and in controls: p = 0.37 for D, p = 0.72 for D*, and p = 0.80 for f.

Discussion

Young Fontan patients in this study had good post-operative hemodynamics. Although all patients showed almost normal liver function by laboratory testing and liver ultrasonography, intravoxel incoherent motion imaging parameters were significantly decreased compared to age-matched healthy controls. This suggests that intravoxel incoherent motion imaging may detect a pre-fibrotic liver state in young Fontan patients with good hemodynamics.

Lu et al showed decreased D value in adult liver fibrosis compared to healthy volunteers.[22] A decreased D value in chronic liver disease reflects an increase in connective tissue, which changes the cell density and histological structure.[19] D* and f values are surrogate markers of capillary liver perfusion.[10] A decreased D* or f value reflects decreased capillary perfusion. Despite increased cardiac output and circulating blood volume, called hyperdynamic circulation,[23–25] decreased liver perfusion exists in liver cirrhosis with normal heart structure.[10,26–29] Consistent with this phenomenon, previous studies have demonstrated a great reduction of perfusion-related intravoxel incoherent motion imaging parameters, D* and f, in fibrotic and cirrhotic livers compared to healthy livers in adults with normal heart structure.[10,16,17,19] Thus, intravoxel incoherent motion imaging is being recognised as a sensitive method to detect structural and perfusion abnormalities in fibrotic and cirrhotic livers in the setting of normal heart structure.

Decreased D, D*, and f values in young Fontan patients in this study were similar to those of liver fibrosis in the setting of normal heart structure. However, these do not necessarily indicate liver fibrosis, especially because D* and f values can be affected by systemic blood flow, which is known to be decreased to 70% (range 50–80%) of normal for body surface area.[30] However, in this study, the D* value in Fontan patients was only 23% of healthy controls, which was much less than the degree of expected reduction in systemic blood flow. This excessive decrease may reflect the capillary perfusion abnormality in Fontan patients. Moreover, the decreased D value in this study cannot be explained by reduced systemic blood flow but does indicate decreased molecular diffusion suggesting a structural change of the liver. Although liver conditions of Fontan patients studied in this study was apparently normal based on laboratory tests and liver ultrasonography, histological liver abnormalities of young Fontan patients with apparently normal liver function have been previously reported. On post-mortem analyses, Schwartz et al and Johnson et al showed hepatic fibrosis even before the Fontan operation in children.[31,32] It can be postulated that the significant decrease in intravoxel incoherent motion imaging parameters in Fontan patients in this study represents both structural and perfusion abnormalities, suggesting a pre-fibrotic state in Fontan patients. Further investigation is required to confirm this hypothesis.

Progressive worsening of intravoxel incoherent motion imaging parameters in Fontan patients has been reported by Dijkstra et al.[21] Sequential intravoxel incoherent motion imaging assessment may be especially useful because it can cancel the effect of hemodynamic status specific to Fontan circulation (ie, reduced systemic blood flow). Moreover, sequential intravoxel incoherent motion imagings do not require intravenous injection of contrast agents and can be safely done owing to non-invasiveness. Intravoxel incoherent motion imaging based on diffusion-weighted imaging sequence can be performed with all up-to-date MRI scanners without much additional time or special equipment. Consequently, a single MRI scan can provide both usual circulation parameters and intravoxel incoherent motion imaging values.

When evaluating liver abnormalities with intravoxel incoherent motion imaging, a mean value through Segments 5–8 rather than a single segment value in D, D*, and f should be used, as the degree of cirrhotic changes in the liver can be heterogeneous in Fontan patients.[33] In this study, the intravoxel incoherent motion imaging values of Fontan patients varied more than those of control group. It may reflect the heterogeneity within the liver in Fontan patients. Moreover, we evaluated the variability of D, D*, and f values through Segments 5–8 in both Fontan patients and controls, and there were no significant differences. This may suggest reproducibility of intravoxel incoherent motion imaging in the liver.

Table 3. Clinical data of Fontan patients.

	Platelet	T-Bil	AST	ALT	GGTP	HA	P-III-P	T4C7 s	BNP	CVP	CI
	(×10⁴/µl)	(mg/dL)	(U/L)	(U/L)	(U/L)	(ng/ml)	(U/ml)	(ng/ml)	(pg/ml)	(mmHg)	(L/min/m²)
Fontan 1	12.2	0.8	36	39	123	26	2.2	9.8	11.5	11	2.97
Fontan 2	27.9	0.3	29	26	52	54	1.4	7.2	55.4	10	2.59
Fontan 3	25.5	0.8	24	19	27	30	2.2	8	6.7	12	2.51
Fontan 4	19.3	0.4	24	27	38	24	0.72	7.8	4	9	2.62
Fontan 5	14.8	1.1	26	21	26	12	1.3	6.5	11.8	9	2.35
Average	19.9	0.68	27.8	26.4	53.2	29.2	1.6	7.9	17.9	10.2	2.61
SD	6.7	0.33	5.0	7.8	40.4	15.4	0.6	1.2	21.2	1.3	0.23
Normal range	(15–40)	(0.4–1.5)	(13–30)	(10–40)	(13–64)	(< 50)	(< 1.0)	(< 6.0)	(< 20)		

ALT = alanine aminotransferase, AST = aspartate aminotransferase, BNP = brain natriuretic peptide, CI = cardiac index, CVP = central venous pressure, GGTP = gamma-glutamyl transpeptidase, HA = hyaluronic acid, P-III-P = procollagen III N-terminal peptide, SD = standard deviation, T4C7s = type IV collagen 7 s, T-Bil = total bilirubin

Table 4. Intravoxel incoherent motion imaging parameter values.

		S5	S6	S7	S8
D (×10⁻³ mm²/second)	Fontan	1.0 ± 0.2	1.0 ± 0.1	1.1 ± 0.0	1.1 ± 0.0
	Control	1.2 ± 0.2	1.2 ± 0.1	1.4 ± 0.2	1.2 ± 0.2
D* (×10⁻³ mm²/second)	Fontan	25.2 ± 21.5	14.5 ± 10.4	19.7 ± 10.5	64.0 ± 110.8
	Control	98.1 ± 22.6	119.7 ± 19.3	102.4 ± 54.3	132.6 ± 70.7
F (%)	Fontan	17.4 ± 4.7	11.8 ± 5.7	14.0 ± 7.1	9.4 ± 3.2
	Control	21.0 ± 3.3	22.5 ± 2.6	24.0 ± 6.1	22.3 ± 4.1
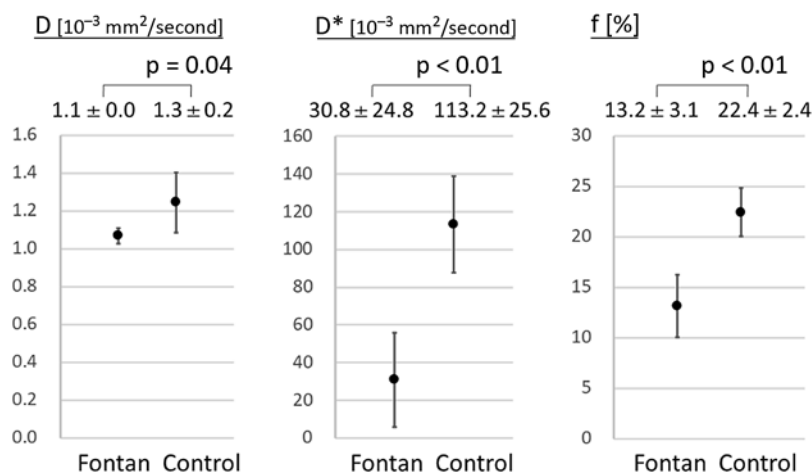
S = Segment

Figure 1. Values of intravoxel incoherent motion (IVIM) parameters. IVIM parameters D, D*, and f in Fontan patients were significantly lower than controls. Each value is the average of Segments 5–8 (Table 4).

This may also be due to the good hemodynamic condition of the Fontan patients. Heterogeneity may become more prevalent with progressive liver disease; moreover, to prevent sample error due to this heterogeneity, we should use a mean value through Segments 5–8 in D, D*, and f.

So far, there have been no well-established quantitative and non-invasive techniques to evaluate liver abnormalities without being affected by central venous pressure. Although liver biopsy is a gold standard for the diagnosis of liver fibrosis, this is an invasive technique with risks of critical complications. Liver stiffness can be assessed quantitatively and non-invasively by transient ultrasound elastography and magnetic resonance elastography. However, elastographies can overestimate the degree of fibrotic change in patients with elevated central venous pressure.[1–4] In the Fontan circulation, systemic venous flow is directly connected to the pulmonary artery bypassing the right ventricle; therefore, a higher central venous pressure than that of normal circulation is prerequisite for establishment of this circulation. Furthermore,

higher central venous pressure results in higher incidence of liver fibrosis and cirrhosis. Therefore, the inability to distinguish high central venous pressure from liver fibrosis is a major limitation of elastography in assessing liver conditions in patients with Fontan circulation. On the other hand, in principle, intravoxel incoherent motion diffusion-weighted imaging is able to detect structural and perfusion abnormalities of the liver without being affected by central venous pressure. In this study, intravoxel incoherent motion imaging was shown to have the possibility to detect pre-fibrotic liver state even in young children with Fontan circulation. Whether or not serial assessment of intravoxel incoherent motion imaging in Fontan patients can distinguish elevation of central venous pressure from development of liver fibrosis in older patients requires further investigation.

There are several limitations to this study. First, a small number of patients were included in this study. Second, age distribution and post-operative duration were limited. Future studies involving more patients with larger hemodynamics variability are warranted. Third, the appropriate fasting time for intravoxel incoherent motion imaging in Fontan patients remain unclear, and 2 hours of fasting time may be too short to evaluate liver perfusion. Fourth, intravoxel incoherent motion imaging parameters were measured only in the right liver lobe, and this may not reflect the overall liver condition. Fifth, no pathological examination was conducted in this study. The standard diagnostic method of liver fibrosis and cirrhosis is pathological examination. However, liver biopsy is an invasive procedure with possible complications.[34] In addition, histological assessment of fibrosis is also an inherently subjective process. The extent of variations from observer interpretation by expert histopathologists may be as high as 20%.[35] Moreover, it is subject to sampling variability due to heterogeneity of liver disease in Fontan patients. Therefore, we thought that it was unsuitable for the diagnosis of early-stage liver abnormalities.

In conclusion, Intravoxel incoherent motion imaging is feasible for evaluating liver abnormalities in children with Fontan circulation. Close observation using intravoxel incoherent motion imaging may be beneficial in these patients.

Author ORCIDs. Kazuhiro Shiraga 0000-0001-7596-0389

References

1. Chon YE, Kim SU, Park JY, et al. Dynamics of the liver stiffness value using transient elastography during the perioperative period in patients with valvular heart disease. PLoS One 2014; 9: e92795.
2. Colli A, Pozzoni P, Berzuini A, et al. Decompensated chronic heart failure: increased liver stiffness measured by means of transient elastography. Radiology 2010; 257: 872–878.
3. Jalal Z, Iriart X, De Ledinghen V, et al. Liver stiffness measurements for evaluation of central venous pressure in congenital heart diseases. Heart 2015; 101: 1499–1504.
4. Millonig G, Friedrich S, Adolf S, et al. Liver stiffness is directly influenced by central venous pressure. J Hepatol 2010; 52: 206–210.
5. Le Bihan D. Intravoxel incoherent motion imaging using steady-state free precession. Magn Reson Med 1988; 7: 346–351.
6. Le Bihan D, Breton E, Lallemand D, et al. Separation of diffusion and perfusion in intravoxel incoherent motion MR imaging. Radiology 1988; 168: 497–505.
7. Le Bihan D, Turner R, MacFall JR. Effects of intravoxel incoherent motions (IVIM) in steady-state free precession (SSFP) imaging: application to molecular diffusion imaging. Magn Reson Med 1989; 10: 324–337.
8. Le Bihan D, Turner R. Intravoxel incoherent motion imaging using spin echoes. Magn Reson Med 1991; 19: 221–227.
9. Annet L, Peeters F, Abarca-Quinones J, et al. Assessment of diffusion-weighted MR imaging in liver fibrosis. J Magn Reson Imaging 2007; 25: 122–128.
10. Luciani A, Vignaud A, Cavet M, et al. Liver cirrhosis: intravoxel incoherent motion MR imaging–pilot study. Radiology 2008; 249: 891–899.
11. Taouli B, Chouli M, Martin AJ, et al. Chronic hepatitis: role of diffusion-weighted imaging and diffusion tensor imaging for the diagnosis of liver fibrosis and inflammation. J Magn Reson Imaging 2008; 28: 89–95.
12. Sandrasegaran K, Akisik FM, Lin C, et al. Value of diffusion-weighted MRI for assessing liver fibrosis and cirrhosis. AJR Am J Roentgenol 2009; 193: 1556–1560.
13. Watanabe H, Kanematsu M, Goshima S, et al. Staging hepatic fibrosis: comparison of gadoxetate disodium-enhanced and diffusion-weighted MR imaging–preliminary observations. Radiology 2011; 259: 142–150.
14. Anderson SW, Barry B, Soto JA, et al. Quantifying hepatic fibrosis using a biexponential model of diffusion weighted imaging in ex vivo liver specimens. Magn Reson Imaging 2012; 30: 1475–1482.
15. Jiang H, Chen J, Gao R, et al. Liver fibrosis staging with diffusion-weighted imaging: a systematic review and meta-analysis. Abdom Radiol (NY) 2017; 42: 490–501.
16. Patel J, Sigmund EE, Rusinek H, et al. Diagnosis of cirrhosis with intravoxel incoherent motion diffusion MRI and dynamic contrast-enhanced MRI alone and in combination: preliminary experience. J Magn Reson Imaging 2010; 31: 589–600.
17. Chung SR, Lee SS, Kim N, et al. Intravoxel incoherent motion MRI for liver fibrosis assessment: a pilot study. Acta Radiol 2015; 56: 1428–1436.
18. Zhang B, Liang L, Dong Y, et al. Intravoxel Incoherent Motion MR Imaging for Staging of Hepatic Fibrosis. PLoS One 2016; 11: e0147789.
19. Zhang J, Guo Y, Tan X, et al. MRI-based estimation of liver function by intravoxel incoherent motion diffusion-weighted imaging. Magn Reson Imaging 2016; 34: 1220–1225.
20. Dijkstra H, Oudkerk M, Kappert P, Sijens PE. Assessment of the link between quantitative biexponential diffusion-weighted imaging and contrast-enhanced MRI in the liver. Magn Reson Imaging 2017; 38: 47–53.
21. Dijkstra H, Wolff D, van Melle JP, et al. Diminished liver microperfusion in Fontan patients: a biexponential DWI study. PLoS One 2017; 12: e0173149.
22. Lu PX, Huang H, Yuan J, et al. Decreases in molecular diffusion, perfusion fraction and perfusion-related diffusion in fibrotic livers: a prospective clinical intravoxel incoherent motion MR imaging study. PLoS One 2014; 9: e113846.
23. Kotelanski B, Groszmann R, Cohn JN. Circulation times in the splanchnic and hepatic beds in alcoholic liver disease. Gastroenterology 1972; 63: 102–111.
24. Groszmann RJ, Vorobioff J, Riley E. Splanchnic hemodynamics in portal-hypertensive rats: measurement with gamma-labeled microspheres. Am J Physiol 1982; 242: G156–160.
25. Vorobioff J, Bredfeldt JE, Groszmann RJ. Hyperdynamic circulation in portal-hypertensive rat model: a primary factor for maintenance of chronic portal hypertension. Am J Physiol - Gastrointest Liver Physiol 1983; 244: G52–G57.
26. Hayashi T, Miyati T, Takahashi J, et al. Diffusion analysis with triexponential function in liver cirrhosis. J Magn Reson Imaging 2013; 38: 148–153.

27. Hu G, Chan Q, Quan X, et al. Intravoxel incoherent motion MRI evaluation for the staging of liver fibrosis in a rat model. J Magn Reson Imaging 2015; 42: 331–339.

28. Ichikawa S, Motosugi U, Morisaka H, et al. MRI-based staging of hepatic fibrosis: Comparison of intravoxel incoherent motion diffusion-weighted imaging with magnetic resonance elastography. J Magn Reson Imaging 2015; 42: 204–210.

29. Wu CH, Ho MC, Jeng YM, et al. Assessing hepatic fibrosis: comparing the intravoxel incoherent motion in MRI with acoustic radiation force impulse imaging in US. Eur Radiol 2015; 25: 3552–3559.

30. Gewillig M, Brown SC, Eyskens B, et al. The Fontan circulation: who controls cardiac output? Interact Cardiovasc Thorac Surg 2010; 10: 428–433.

31. Schwartz MC, Sullivan L, Cohen MS, et al. Hepatic pathology may develop before the Fontan operation in children with functional single ventricle: an autopsy study. J Thorac Cardiovasc Surg 2012; 143: 904–909.

32. Johnson JA, Cetta F, Graham RP, et al. Identifying predictors of hepatic disease in patients after the Fontan operation: a postmortem analysis. J Thorac Cardiovasc Surg 2013; 146: 140–145.

33. Ginde S, Hohenwalter MD, Foley WD, et al. Noninvasive assessment of liver fibrosis in adult patients following the Fontan procedure. Congenit Heart Dis 2012; 7: 235–242.

34. Janes CH, Lindor KD. Outcome of patients hospitalized for complications after outpatient liver biopsy. Ann Intern Med 1993; 118: 96–98.

35. Bravo AA, Sheth SG, Chopra S. Liver biopsy. N Engl J Med 2001; 344: 495–500.